Alternative oxidase activity and vacuolar intrusion of mitochondria represent a delayed mitophagy associated with the chilling stress in *Haberlea rhodopensis*

Áron Keresztes[1], Éva Sárvári[2], Péter Nyitrai[2], Hong-Diep Pham[2×], Gergana Mihailova[3], Gabriella Szalai[4], László Sass[5], Katya Georgieva[3], Imre Vass[5], Ádám Solti[1]*

[1]Department of Plant Anatomy, Institute of Biology, ELTE Eötvös Loránd University, Hungary
[2]Department of Plant Physiology and Molecular Plant Biology, Institute of Biology, ELTE Eötvös Loránd University, Hungary
[3]Institute of Plant Physiology and Genetics, Bulgarian Academy of Sciences, Bulgaria
[4]Agricultural Institute, HUN-REN Centre for Agricultural Research, Hungary
[5]Institute of Plant Biology, HUN-REN Biological Research Center, Hungary

×current affiliation: International University – Vietnam National University, Ho Chi Minh City, Vietnam

*email: adam.solti@ttk.elte.hu

Abstract

The resurrection plant *Haberlea rhodopensis* exhibits tolerance to both desiccation and sub-zero temperatures. While the overlap between the tolerance to desiccation and sub-zero temperatures has been previously described, specific responses to above-zero chilling stress remained poorly understood. Mitochondrial alternative oxidase (AOX) activity is associated with chilling stress tolerance, particularly in plants of (sub)tropical origin, the function of which has not been well resolved in the chilling stress tolerance of resurrection plants. In *H. rhodopensis* leaves naturally exposed to chilling conditions, transcript abundance, protein level, and respiration activity of AOX significantly increased. Ultrastructural analysis revealed that chilling conditions resulted in the intrusion of the vast majority of mitochondria into the central vacuole, where mitochondria were represented in multiple cross sections resembling to immersion heaters. Ultrastructure analysis revealed that mitochondria intruding into the vacuole undergo a gradual degradation process thus considered as mitophagy. In consequence in leaves naturally exposed to sub-zero conditions, the degradation of the vacuole intruding mitochondria is nearly complete associated with a decreased AOX activity and protein amount. Leaf temperature alterations under chilling conditions and after sub-zero conditions support the heat generation based on the increased AOX activity under chilling conditions. Our findings revealed an adaptive strategy in *H. rhodopensis* to chilling conditions, where coordinated AOX-driven respiration and delayed mitophagy, enabling a temporal existence of mitochondria intruded into the vacuole together support metabolic stability.

Keywords: alternative oxidase; mitochondria; respiration; thermogenesis; vacuole

Highlights:

- Mitochondria intruding into the vacuole appear in *H. rhodopensis* under chilling
- Increased AOX activity co-occur with vacuole intruded mitochondria
- Mitophagy is only completed after subjected to sub-zero temperatures
- Existence of mitochondria intruded into the vacuole represents a delayed mitophagy
- Delayed mitophagy is suggested as a chilling stress tolerance mechanism

1. Introduction

Plants, the majority of which are sessile, are prone to all the effects of their changing environment and developed widespread protective mechanisms to survive stressful conditions. Resurrection plants represent unique organisms that tolerate the stressful environment, such as the loss of cellular water content by anabiosis. Homoichlorophyllous resurrection angiosperm *Haberlea rhodopensis* (Gesneriaceae), interglacial relic taxon of a (sub)tropical kinship, colonise rock rifts in the Balkan and Rhodope Mountains. In contrast to certain resurrection angiosperms of (sub)tropical origin, this taxon survives not only water deficit periods but also the sub-zero temperatures during winters, while retaining photosynthetic apparatus and chlorophyll content (Georgieva et al., 2020; Mihailova et al., 2020; 2023; Legardón and García-Plazaola, 2023). To sustain these extremes, leaves lose 90-95% of water content, which is substituted by soluble sugars (mainly sucrose) with a concomitant rearrangement of intracellular structure and ceased metabolic activity (Mihailova et al., 2020) in the mesophyll cells. At drought or sub-zero temperatures induced desiccation, multitudinous defence mechanisms were identified including photoprotection, expression of stabilizing proteins and metabolites, and enhanced antioxidative protection (Solti et al., 2014; Mladenov et al., 2022; Georgieva et al., 2022; Legardón, García-Plazaola, 2023). Over *Ramonda* spp. (s.l.) the close relatives of *H. rhodopensis* are of tropical and subtopical origin (tribe Trichosporeae, subfamily Didymocarpoideae), whereas *H. rhodopensis* is among the few taxa that has been adapted to survive temperate, high mountain climate. Although Mihailova et al. (2020; 2023) indicated that certain chilling stress tolerance mechanisms overlaps with that of the desiccation, responses of *H. rhodopensis* to chilling temperatures are generally hardly documented. Though previous studies documented changes in the metabolome and basic physiological parameters under low temperature stresses (Benina et al., 2013; Georgieva et al., 2021, 2022; Mihailova et al., 2020; 2023), these studies have emphasised the differences among chilling (above zero) and sub-zero conditions responses.

The mitochondrial alternative electron transport pathway has been shown to activate in different stresses, including chilling stress (Vanlerberghe, 2013, 2020; Pu et al., 2015; Saha et al., 2016; Del-Saz et al., 2018). Although mitochondrial activity is fundamental to ensure carbon intermediates for the synthetic processes and to control the NADPH and ATP levels in the different cell compartments by the malate/citrate valves and the ratio of the cytochrome pathway to alternative electron transport (Igamberdiev, 2020; Vanlerberghe et al., 2020), mitochondria also have a pivotal role in photosynthetic plant cells in balancing the energy metabolism (Laxa et al., 2019; Considine and Foyer, 2023). In the alternative route, excess

reducing power can be removed without generating a transmembrane proton gradient and thus ATP by alternative terminal oxidases (AOX), while the energy is being released as heat (Vanlerberghe, 2013; Rogov et al., 2014). AOX proteins are 32-36 kDa dimeric non-heme di-iron carboxylate enzymes bound to the matrix side of the inner mitochondrial membrane. Their activity is cyanide-resistant but inhibited by hydroxamic acid (Schonbaum et al., 1971). AOXs, derived from the endosymbiosis by alpha-proteobacteria are related with chloroplast terminal oxidases (PTOX) of cyanobacterial origin. By early gene duplication in the green plant lineage, AOX1 and AOX2 type enzymes exist in dicots (Selinski et al., 2018). *AOX1* and *AOX2* gene families are encoded by the nuclear genome and usually co-expressed with alternate dehydrogenases (Clifton et al., 2005; Ho et al., 2007). The role of AOXs is particularly important in stress tolerance (Saha et al., 2016) including chilling stress: both the expression and the activity of AOXs generally elevates at low temperature (Grabelnych et al., 2014; Mroz et al., 2015; Karami-Moalem et al., 2018), with few opposite examples (Heidarvand et al., 2017). The connection between the chilling stress tolerance in plants, particularly that of tropical and subtropical origin has been well established (*Nicotiana tabacuum*: Wang et al., 2011; *Oryza sativa*: Li et al., 2013; *Cucumis sativus*: Mróz et al., 2015; *Ipomea batatas*: Zhang et al., 2021; *Gossypium hirsutum*: Pham et al., 2018). Hendrickson et al. (2019) also showed on *Pyrus communis* fruits that pre-conditioning under cold conditions increases the later low temperature stress that is connected with the higher expression and activity of AOX. It is also known that chilling stress enhances the synthesis of regulatory substances like nitric oxide, ethylene, and salicylic acid (SA) that impact the expression of the *AOX* genes (Ho et al., 2007; 2008). The significance of heat released in the mitochondrial alternative electron transport pathway is mainly supported in thermogenic plants where the heat produced during flowering liberates insect-attractive aromatic compounds (Meeuse, 1975; Lamprecht et al., 2002; Miller et al., 2011). Although its importance in non-thermogenic plants is often debated (Breidenbach et al., 1997; Grabelnych et al., 2003), AOX activity was shown to be essential in the survival of severe drought stress in non-resurrection *Nicotiana tabacum* (Wang and Vanlerberghe, 2013). In *H. rhodopensis,* Ivanova et al. (2022) showed that the AOX-mediated alternative mitochondrial respiration also has a fundamental role in the desiccation tolerance, especially under rehydration where mitochondrial function restores prior to photosynthesis. Although general low temperature tolerance mechanisms with that of desiccation tolerance (Mihailova et al., 2020; 2023) the chilling stress responses of *H. rhodopensis* has not been clarified yet.

Autophagy is a specific action of eukaryotic cells resulted in a selective removal of cell components. Mitochondrial autophagy (mitophagy) specifically targets mitochondria by

controlling their number in the cells and eliminates damaged organelles upon stress conditions (Minibayeva et al., 2012). Although earlier studies claimed that evidence for neither the autophagosome mediated nor the direct uptake and subsequent degradation (macro- and microautophagy, respectively) of mitochondria existed (van Doorn and Papini, 2013; Broda et al., 2018), Nakamura et al. (2021) proved the existence of mitophagy in plant cells. Important to note that autophagy is generally a rapid process that is hard to investigate. Zhu et al. (2018) have demonstrated that ROS signalling derived from AOX activity is essential in initiating autophagy, which has a pivotal role in a sufficient response to drought stress. On the other hand, Kacprzak and van Aken (2022) reviewed that stresses that affect mitochondria also trigger mitophagy. In general, depolarization of the mitochondrial membranes is a trigger of mitochondrial degradation, in plant cells, too (Otegui et al., 2024). Due to the existence of mitochondrion-specific cargo receptors, autophagy is the way of degradation of mitochondria in plant cells (Luong et al., 2022; Petersen et al., 2024).

In this study, we present structural and functional characteristics of mitochondria in *H. rhodopensis* leaves concluding that AOX activity has important role in the chilling stress response. Chilling stress also resulted in an intrusion of multiple mitochondria into the vacuoles that status was persisting in time long enough for an accumulation of these structures. Taken into consideration the rapid elimination of these structures upon an exposure to sub-zero conditions, the persisting vacuolar intrusion of the mitochondria was considered as a delayed mitophagy situation. Co-occurrence of the vacuolar intrusion of the majority of the mitochondria with the increased mitochondrial AOX activity suggest the importance of the structure in the chilling stress tolerance.

2. Materials and methods

2.1 Plant material

Haberlea rhodopensis Friv. plants originated from the Rhodope Mountains, Bulgaria, were cultivated according to the environmental conditions of the natural vegetation in the *ex-situ* protected plant collection of the Botanical Garden, Eötvös Loránd University, Budapest, Hungary (47°29'05.2"N 19°05'06.2"E). Plants were kept in shade below tree canopy where average peak light intensity was between 20 and 30 µmol photons m^{-2} s^{-1} photosynthetic photon flux density (PPFD) in October. Mature leaves (that has finished the area expansion) of adult rosettes of similar size were selected for the experiments. Leaves in the same physiological status of identical rosettes, belonging to the same ramet were employed in each sampling point.

In addition, to minimise the number of the leaves to be sampled, all *in vivo* measurements were accomplished before sampling from the identical leaves for analysis. To determine SA content and respiration activity, multiple leaves in the same physiological status of the rosette, or multiple leaves of the same ramet was applied. Leaves were collected prior to temperature stress period in early October (BS – before stress), under chilling stress conditions in November and in December (CH), after frost conditions in January and in February (SZ – sub-zero) and after the temperature stress period in April (AS – after stress). At transferring leaf material from the *ex situ* cultivation site to *in vivo* laboratory measurements, the biological material was carried in temperature protecting box, adjusted to the environmental temperature previously. Samples for expression analysis, immunoblotting, and SA determination were frozen in liquid nitrogen and stored at -80 °C. Samples for ultrastructure analysis were collected and fixed at the *ex situ* cultivation side under environmental temperature.

2.2 Environmental and leaf temperatures

Minimum and maximum temperature values were recorded by an analogous mercury-in-glass minimum/maximum thermometer, measurement range of -20 – +50 °C, accuracy ±1 °C. Minimum and maximum temperature values were recorded 9 am, every morning. Leaf temperature was measured using the NiCr-Ni thermocouple in the head of a PAM 2500 (Walz, Germany) device, measuring range -5 °C to +40 °C, accuracy ±0.5 °C (in the 0 °C to +25 °C range) contacting the abaxial surface of the leaves. Temperature in the proximal environment of the leaves was recorded by a digital thermometer (30.5007, TFA Dostmann, Wertheim-Reicholzheim, Germany) of measuring range -10 – +50 °C, accuracy ±1 °C.

In order to record the fine-scale temperature of the leaves of plants kept under *ex situ* garden conditions, a pilot recording was performed in the winter 2017/2018 by registering the leaf and the environmental temperature applying a sensitive thermocamera (Varioscan 3021ST, Jenoptik, Germany; 0.03 °C resolution; sensitivity range for infrared radiation in the 8–12 μm wavelength interval; Kaňa and Vass, 2008). Ambient temperature information was collected on a reference surface staying in thermal equilibrium with the ambient temperature. Thermal images were analysed by using ImageJ.

2.3 Chlorophyll a fluorescence induction

To characterise the status of the photosynthetic apparatus as non-invasive indicator, excitation energy allocation was determined by chlorophyll *a* fluorescence induction using a portable chlorophyll *a* fluorometer (Barócsi et al., 2009). Excitation energy allocation, modelled as

effective quantum efficiency of photosystem (PS)II reaction centres (Φ_{PSII}), thermal emission of the PSII antennae (Φ_{NPQ}), energy dissipation of the non-functioning PSII reaction centres (Φ_{NF}), and excitation energy dissipated in the form of fluorescence and constitutive thermal dissipation ($\Phi_{f,D}$) were calculated as in Solti et al. (2016).

2.4 Electron microscopy

Leaf pieces were fixed under *ex situ* environmental conditions in 2.5% (w/V) glutaraldehyde (65 mM K–Na phosphate buffer, pH 7.2) for 2 h, at external temperature, *in situ*. After thorough washing with the buffer, samples were post-fixed in 1% (w/V) OsO_4 for 1.5 h, followed by dehydration in ethanol series and embedding in Durcupan ACM. Samples were sectioned with an ultramicrotome (Ultracut E, Reichert-Jung) and then stained with uranyl acetate and lead citrate. The sections were examined in a Hitachi 7100 (Hitachi Ltd, Tokyo, Japan) electron microscope. Micrographs were taken with a MegaView III camera (Soft Imaging System, Münster, Germany).

2.5 Identification of *H. rhodopensis* sequences

Based on the detailed sequencing study and contig analysis of Gechev et al. (2013) contigs associated with mitochondrial alternative oxidase (contigs 002889, 008063, 021324 and 042667) were analysed and all found encoding orthologues sequences to *At5g64210* (mitochondrial alternative oxidase *AtAOX2*). Contig 002889 (*HrAOX2*; 72 nucleotides overlap to *At5g64210* between nucleotides 350–922; Waterman-Eggert score: 1488, $8.5e^{-48}$, identity/similarity: 73.3%, gap: 0 [0%]) were chosen for further expression analysis. As for reference genes, orthologues of heat shock protein 90 and ubiquitin conjugase were searched and found as contigs 000452 (*HrHSP90*, 514 nucleotide overlap to *Arabidopsis lyrata XP_002869603* between nucleotides 1903–2416; Waterman-Eggert score: 1688, $6.4e^{-44}$, identity/similarity: 80.9%, gap: 0 [0%]) and 009712 (*HrUBC5*, overlap to *At3g62250* between nucleotides 370–737; Waterman-Eggert score: 721, $4.1e^{-23}$, identity/similarity: 67.1%, gap: 18 [5%]) in the contig database.

2.6 Expression analysis

Approximately 100 mg of fresh leaf stored in liquid nitrogen was subjected to total RNA extraction using TRI Reagent® (Sigma). Samples homogenized in 1 ml of TRI Reagent and 0.2 ml chloroform were used to phase separate mRNA according to the manufacturer's instructions. Nucleic acid pellet was washed in 75% ethanol, dried at RT, and dissolved in 50 µl diethyl-

pyrocarbonate-treated water. RNA concentration was quantified by a Nanodrop ND-1000 (Thermo-Fisher Scientific Inc., Waltham, MA, USA). Residual genomic DNA contamination was eliminated by RNase-free DNase I (Thermo-Fisher Scientific) treatment. Reverse transcription of the RNA pool was performed using random hexameric oligonucleotides by RevertAid Reverse Transcriptase (Thermo-Fisher Scientific) according to the manufacturer's instruction. The cDNA libraries were stored at -80 °C to further applications.

To study the relative expression of *HrAOX2* based on the reference genes *HrHSP90* and *HrUBC5*, specific oligonucleotide primers were designed according to Table 1. All target primer pair sequences amplified single PCR products of expected sizes with optimal annealing temperature and primer concentration. Efficiencies were estimated and qPCR reactions were performed by StepOnePlus Real-Time PCR system (Applied Biosystems) and evaluated with the StepOne™ v.2.2.3 software. The primer specificity was confirmed by the presence of a sharp peak during melt curve stage together with 2% agarose gel electrophoresis of PCR products. A standard curve was generated using 7 points of twice-fold serial dilutions of cDNA template to calculate the PCR efficiencies of target genes. Efficiency of each gene was estimated from the slope of a linear regression model and ranged from 1.95–2.05.

To identify the differential expressions among samples by qPCR, 100× diluted cDNA samples, 0.15–0.5 µM gene specific primers and 2× diluted SYBR Green reagent (Luminaris Color HiGreen High ROX, Thermo-Fisher Scientific) were used in the final volume of 15 µl. All cDNA samples were freshly diluted before qPCR reactions. All measurements were repeated on three technical replicates. The qPCR program was set up as follows: a predigest step of 50 °C for 2 min, a 95 °C initial denaturation step for 10 min, 40 cycles of 95 °C for 15 s (denaturation), T_m for 20 s (annealing), 72 °C for 20 s (extension), and final melt curve stage. Quantification of the normalized relative transcript level of specific genes was performed according to the method of Pfaffl (2001).

2.7 Immunoblotting

Approximately 50 mg leaf samples were homogenized in 1 ml of 62.5 mM Tris-HCl (pH 6.8), 2% (w/V) SDS, 2% (w/V) DTT, 8.7% (w/V) glycerol. The mixture was incubated at room temperature for 30 min. The non-solubilised material was removed by centrifugation at 10,000 $\times g$ for 5 min, and 0.001% (w/V) bromophenol blue was added. Solubilized proteins were separated by SDS PAGE on 10–18% gradient acrylamide gels (Laemmli, 1970 but containing 8.7% (w/V) glycerol) in a MiniProtean apparatus (BioRad) using a constant current of 20 mA per gel (surface 1 cm^2) at 6 °C. Proteins were transferred to Amersham™ ProtranTM Premium

0.2 µm nitrocellulose blotting membranes (GE Healthcare) in 25 mM Tris (pH 8.3), 192 mM glycine, 20% (V/V) methanol and 0.02% (w/V) SDS at 6 °C using constant voltage of 90 V for 3 h.

Immunoblots against mitochondrial alternative oxidase was performed with rabbit polyclonal antibody against fully conserved C-terminal consensus motifs of *Arabidopsis thaliana*, *Solanum lycopersicum*, and *Oryza sativa* mitochondrial alternative oxidase isoforms (AOX1/2; AS04 054; Agrisera AG, Vännäs, Sweden). For positive control/band identification, leaf total proteins of *Typhonium venosum* (Dryand. ex Aiton) Hett. & P.C.Boyce (syn. *Sauromatum guttatum* Schott) synandrium (inflorescence) and adult rosettes of *Arabidopsis thaliana* (L.) Heynh. 'Col-0' grown at 4 °C for two-week time were used. Antibodies were dissolved in 20 mM Tris-HCl (pH 7.5), 0.15 M NaCl, 1% (w/V) gelatine following the manufacturer's instructions. Horseradish peroxidase-conjugated goat-anti-rabbit IgG (BioRad) was used to detect bands following the manufacturer's instructions. The amount of AOX proteins was counted by comparing the area density in the different samples using Phoretix 4.01 software (Phoretix International, Newcastle upon Tyne, UK). The normalization of protein quantification was based on the total leaf protein basis.

2.8 Determination of salicylic acid and derivatives

SA extraction and analysis were performed according to Pál et al. (2005). After separation on a reverse phase column (Synergi Fusion-RP, 80 A, 150×4.6 mm, 4 µm, Phenomenex, Inc., CA, USA), SA and SA conjugates were quantified fluorimetrically (W474 fluorescence detector, Waters, USA, excitation: 305 nm; emission: 407 nm).

2.9 Respiration capacity

In order to measure respiration, leaves were transferred to the laboratory under the same environmental temperature. Leaf discs of 3.8 cm^2 were used in oxygen consumption measurements. To inhibit respiratory pathways, 5 µM NaN_3 (99.5%, Sigma-Aldrich, inhibitor of the mitochondrial terminal oxidation; Fedoseva et al., 2008) and/or 1 mM salicylhydroxamic acid (SHAM, 99%, Alfa Aesar, inhibitor of the mitochondrial alternative oxidase; Seyran et al., 2010) were used. Respiratory inhibitors were infiltrated in 20 ml 50 mM HEPES-KOH, pH 7.0, 330 mM sorbitol, 2 mM $MgCl_2$, 2 mM EDTA buffer under vacuum by shaking for 15 min. Respiration intensity of leaf discs was measured by Hansatech Oxylab (Norfolk, UK) oxygen electrode. Measuring temperatures of material originating from different environmental conditions, the temperature was adjusted by thermostat to 20 °C (BS, AS) and to 5 °C (CH,

SZ), respectively. The respiration capacity of the alternative pathway (R_{alt}) is given as the difference of O_2 consumption without inhibitors and in the presence of 5 µM NaN_3 plus residual respiration (R_{res}). R_{res} is given as O_2 consumption in the presence of both 5 µM NaN_3 and 1 mM SHAM. The respiration capacity of the cytochrome pathway (R_{cyt}) is given as the difference of O_2 consumption without inhibitors and in the presence of 1 mM SHAM plus R_{res}.

2.10 Samples and statistical analysis

The experiments were repeated in three subsequent years on biological samples cultivated under environmental conditions. Before sample collecting, physiological parameters were recorded under *ex situ* garden conditions. For microscopy analysis, 3 leaves of different plant individuals were sampled in two subsequent years, in the winters of 2013/2014 and 2014/2015. Samples for transcript and protein analysis were taken in all three subsequent years and processed in 3 technical replicates on 3 biological replicates per sampling point. Respiration measurements were performed on 3 leaf disks of different plant individuals per sampling in two subsequent years, in the winters of 2014/2015 and 2015/2016. To extract metabolites for the analysis of salicylic acid derivatives, a sum of 1 g fresh leaf material, collected from multiple plant individuals and in all three subsequent years were applied per sampling. Comparing variance between groups by one-way ANOVAs with Tukey–Kramer *post hoc* tests and analyse correlation by Pearson R assuming Gaussian distribution of the dataset were performed using Graphad Prism v.9.2 (GraphPad software Inc., USA). The term significantly different refers to a similarity of samples of $P < 0.05$.

3. Results

3.1 Environmental conditions and physiological status

The plant material was grown under *ex-situ* garden conditions. Since the experimental site was located in Hungary, Central Europe, plants were naturally exposed to gradual decline in the light hours and intensity of the solar irradiation as well as chilling and sub-zero conditions typical to temperate climate (Suppl. Fig. 1; Suppl. Dataset 1). The physiological experiments and sample collecting were performed in three subsequent years, the winters of 2013/2014, 2014/2015 and 2015/2016, in which three years the pattern of the minimum and maximum, as well as the daily average temperatures followed matching tendencies (Table 2). According to the changes in the temperature parameters, *in vivo* measurements and sample collecting were performed on BS conditions on the 23rd October, on the 14th October and on the 7th October; under CH conditions on the 18th December, on the 25th November and on the 24th November;

under SZ conditions on the 4th of February, on the 8th January and on the 4th January; and under AS conditions on the 10th of April, on the 15th April and on the 19th April in 2013/2014, 2014/2015 and 2015/2016, respectively (Suppl. Fig. 1). In parallel to decrease in the environmental temperature, the effective quantum efficiency of photosystem II (PSII) reaction centres (Φ_{PSII}) decreased under CH (Fig. 1) resulting in the allocation of the majority of the excitation energy in the form of thermal emission of the PSII antennae (Φ_{NPQ}). In SZ samples, in contrast to CH, a complete inactivation of PSII reaction centres occurred resulting in the increase in the energy dissipation of the non-functioning PSII reaction centres (Φ_{NF}) together with an increase in the excitation energy dissipated in the form of fluorescence and constitutive thermal dissipation ($\Phi_{f,D}$). In parallel with the rising temperatures in the spring, the excitation energy allocation restored in AS leaves to the values of BS samples.

3.2 Leaf temperature

Prior to CH conditions, the leaf temperature is BS leaves was lower compared to the ambient temperature. In CH sampling points, regardless of the sampling year but depending on the ambient temperature, the leaf temperature increased compared to the ambient temperature (Fig. 2). The difference between leaves to ambient temperature was significantly higher at lower environmental temperature, reaching a maximum when the leaves were first exposed to sub-zero temperatures (SZ-1), whereas after multiple days of sub-zero exposure , the temperature of the leaves did not differ from the ambient temperature. In AS sampling points the temperature of the leaves was slightly elevated compared to the ambient temperature.

To analyse the alterations in the leaf temperature, a detailed analysis was performed using high sensitivity thermal camera in the 12 °C to -1 °C ambient temperature range. Regardless the date of the data collecting the maximum temperature pixels on the leaves indicated a significant negative correlation to the ambient temperature reference (n = 17; Pearson R of 0.5842; two-tailed P of 0.0138, significant), whereas the minimum and average temperature pixels showed no correlation to the ambient temperature (Fig. 3A). In the deviation of maximum temperature pixels to the average leaf temperature (Fig. 3B), a remarkable significance was recorded (n = 17; Pearson R of -0.7790; two-tailed P of 0.0002, extremely significant). As a tendency, minimum and maximum leaf temperature pixels were identified on the basal and on the apical part of the leaf lamina, respectively (Fig 3C-F).

3.3 Ultrastructure of mesophyll cells

In BS samples, a general arrangement of mesophyll cells was observed: organelles were located at the cell periphery, and one large vacuole filled most of the cell volume. In CH samples of December, 2013, the vast majority of mitochondria were seen intruded into the central vacuole, while a few were found in the cytoplasm (Fig. 4A). Mitochondria in the vacuole were connected to each other by electron dense layers (Fig. 4A and B). Some of these mitochondrial profiles were roundish or elongated, whereas others were curved or forming ring-like structures in section (Fig. 4B). Vesicles presumably originating from the tonoplast could be seen around several mitochondrial sections (Fig. 4B). In CH samples of November, 2014, a central vesicle presumably of inner membrane origin appeared in mitochondria, while in others the matrix appeared to be inflated, thinned, and these structures showed signs of degradation (Fig. 4C). In SZ samples, regardless of the sampling year, all organelles appeared toed from the plasma membrane, and were surrounded by smaller or larger secondary vacuoles in the cell interior. The few cytoplasmic mitochondria in the vicinity of the roundish chloroplasts remained structurally intact (Fig. 4D). In AS samples, regardless of the sampling year, ultrastructure resembling that of in BS samples was found.

3.4 Salicylic acid in the leaves

In BS samples, both free and bound SA were detected (Fig. 5). In CH samples, the dry weight based free SA content elevated significantly compared to BS ones, but no difference was measured in the amount of bound SA content. In SZ samples, the dry weight-based content of free SA decreased and was even lower than in BS ones. However, the amount of bound SA increased significantly compared to both BS and CH samples. In AS samples, the free SA content was similarly low as in SZ ones and that of the bound SA did not differ significantly from that of in BS samples.

3.5 Expression of the mitochondrial alternative oxidase

The relative transcript abundance of the mitochondrial alternative oxidase *HrAOX2* indicated significant alterations in samples collected under different temperature conditions and periods of the winter (Fig. 6A). In CH samples, the relative transcript abundance was approximately three-fold higher compared to that in BS ones. SZ samples, the relative transcript abundance of *HrAOX2* was still high and showed no difference compared to that in CH ones. Nevertheless, in AS samples, the relative transcript abundance of *HrAOX2* was low, even lower than that of in BS samples.

3.6 Protein amount of the mitochondrial alternative oxidases

Total proteins were isolated from *H. rhodopensis* leaves. Immunoblot analysis of the solubilised protein samples applying anti-AOX 1/2 IgG indicated the presence of one single AOX band in *H. rhodopensis* leaves, in contrast to *Arabidopsis thaliana* leaves subjected to chilling stress, where two bands of different MWs appeared (Fig. 6B). Using *Typhonium venosum* synandrium as a positive control, the single band resembling the MW of that in *H. rhodopensis* samples was identified. Thus, the presence of AOX proteins was confirmed in *H. rhodopensis* leaves.

In CH samples, a tendency of alteration in the relative amount of AOX proteins, similar to that of in the expression of *HrAOX2* was observed. In consequence the relative amount of AOX proteins increased significantly, approximately doubled in CH samples compared to that of in BS ones (Fig. 6C). In SZ samples, the intensity of the AOX band decreased compared to that in CH samples, difference is not significant. In AS samples, the AOX band intensity was lower, the difference was not significant compared to that of in BS samples.

3.7 Oxygen consumption

To differentiate between the cytochrome c oxidase dependent oxygen consumption and the oxygen consumption of the AOX-type alternative terminal oxidases, the respiration was measured under the effect of selective inhibitors NaN_3 and SHAM, respectively, allowing the calculation cytochrome c oxidase dependent pathway, R_{cyt} and that of the AOX-dependent pathway, R_{alt} to the respiration. Under CH conditions, R_{alt} increased significantly compared to that in BS samples, whereas in SZ amples R_{alt} decreased compared to that of in CH samples (Fig. 7). R_{alt} did not differ significantly in BS and AS samples. In comparison to R_{alt}, the R_{cyt} did not increase under CH conditions compared to that of in BS samples. In SZ samples, R_{cyt} was lower compared to that of in AS.

4. Discussion

H. rhodopensis is able to survive chilling stress and sub-zero conditions where tolerance mechanisms against low temperature stresses, especially that of against frost stress and desiccation tolerance highly overlap (Mihailova et al., 2020; Georgieva et al., 2021; Georgieva et al., 2022; Mihailova et al., 2022). Regarding tolerance mechanisms against sub-zero temperstures, Mihailova et al. (2020) described that few day sub-zero environmental temperature resulted a rapid water loss, and thus desiccation in the foliage. Thus, the tolerance mechanisms of sub-zero temperatures and the desiccation overlap. However, except the chilling

stress conditions (CH in the current study), we have not observed mitochondria intruded into the vacuole under other stress conditions. A typical response of the plant taxon to desiccation stress is the formation of secondary vacuoles that replaces the primary vacuole and resulting in a highly vacuolated ultrastructure in the desiccated stage (Georgieva et al., 2017). These secondary vacuoles also appear after leaves were subjected to sub-zero conditions, as appears on Fig. 4D. Under low temperature stress, elevated levels of carbohydrates, proline, dehydrins and ELIPs (Benina et al., 2013; Georgieva et al., 2022), polyphenols, and increased activity of antioxidant enzymes (Georgieva et al., 2021**)** were detected previously. These chilling stress adaptation processes are also documented in the various angiosperm species (Verhoeven et al., 2018). Regarding the energy producing processes in *H. rhodopensis*, decline of PSII activity and an elevated cyclic electron flow in the photosynthetic electron transport was previously demonstrated (Mihailova et al., 2020). However, tolerance mechanisms against chilling stress and sub-zero temperatures have not been distinguished yet. Under chilling stress conditions, our results showed a significantly increased R_{alt} capacity. Moreover, the primary excitation energy allocation of the PSII shifted from the function of PSII photochemistry towards the excitation energy quenching of the PSII antennae. Whereas in samples subjected to sub-zero temperatures, the R_{alt} capacity was still higher than in stages not affected by low temperature stress, the inactivation of PSII reaction centres became nearly complete, similar to our previous results (Mihailova et al., 2020). In consequence, under chilling stress and the effect of sub-zero temperature, the photosynthetic activity is suppressed, similarly to the terminal stage of desiccation in *H. rhodopensis*. Cheng and Zhang (2021) indicated that the activation of AOX protected PSI acceptor side by the malate–oxaloacetate shuttle, thus contributing to the balance of the electron transport in chloroplasts. However, recent results of Yamada et al. (2024) referred that AOX activity rather impacted PSII activity under low temperature stress. Restoration of the mitochondrial respiration is also among the first processes during the rehydration of *H. rhodopensis* (Ivanova et al., 2022).

Respiration is generally more tolerant to low temperature stress than photosynthesis (Mathur et al., 2014). Moreover, enhancing the AOX-dependent alternative terminal oxidation in mitochondria is also a general response to chilling stress in tolerant species (Wang et al., 2014). AOX activity is generally important in the chilling stress tolerance of the vegetative tissues and fruits, and thus *Haberlea rhodopensis* is not an exception but accommodates to the general trend. Nevertheless, the novelty of our study that also represent a unique ultrastructure for the *H. rhodopensis* is that the high AOX expression, protein amount and activity co-occurred with the intrusion of mitochondria into the vacuoles. Taking into account the abundance of

mitochondrial structures in the cytoplasm versus those intruded into the vacuoles, the coincidence underline that high AOX activity is connected to the vacuolar intrusion of mitochondria in *H. rhodopensis*. Since in SZ samples both the AOX activity and protein amount decreased, together with the elimination of vacuole intruded mitochondria, the connection is even more supported. In response to CH conditions we have also measured a significant increase in R_{alt} supported by the increased expression of *HrAOX2* and the enhanced amount of AOX proteins. The amount of free SA that is involved in the triggering of the expression of *AOX* genes in both *Arabidopsis thaliana* and *Nicotiana tabacum* (Ho et al., 2008; Cvetkovska and Vanlerberghe, 2012) also accumulated in leaves of *H. rhodopensis* under chilling conditions, supporting the strong enhancement of the AOX-dependent alternative terminal oxidation in mitochondria. In consequence, under CH conditions, the activation of R_{alt} in *H. rhodopensis* was a similar response to chilling stressed angiosperms (Zhang et al., 2021; Jiang et al., 2023). In parallel with the strong induction of AOX dependent respiration, no activation, but rather a slight decrease of the cytochrome oxidase pathway was measured in the current studies, indicating a massive shift in the function of mitochondria in *H. rhodopensis* leaves. In spite of the usual decrease in CO_2 fixation activity by the lowered temperature (Yamori et al., 2014), the malondialdehyde content referring to ROS production only slightly elevated under CH conditions (Georgieva et al., 2022) as a result of of cyclic electron transport (Mihailova et al., 2020). These data shown strong connections to the increased AOX activity found in the current study.

Under CH conditions, the temperature of *H. rhodopensis* leaves increased compared to the local environment. Though oxygen consumption of folding *H. rhodopensis* leaves cannot be mapped in high resolution, our thermal camera imaging revealed a spatial distribution difference in the leaf temperature where the highest maximum leaf temperature values were recorded on the apical part of the leaf lamina (Fig. 3). Mihailova et al. (2020) described that desiccation was a general response of *H. rhodopensis* to low temperature stress, in which process the water loss through epidermal pores had an importance. Considering that desiccation of the leaf lamina in *H. rhodopensis* is not homogenous where the desiccation and folding of the apical part of the lamina precedes that of the basal region and that mitochondrial alternative respiration is upregulated and thus has a pivotal importance in the terminal phase of the desiccation (Ivanova et al., 2022), the leaf lamina location of elevated temperature compared to the environment may correspond to the high mitochondrial AOX activity. Regarding the possibilities of AOX-induced temperature elevation in non-thermogenic tissues, Vojnikov et al. (1984) already reported on elevated temperature of wheat (*Triticum aestivum*) shoots under chilling stress,

accompanied by an increase in the oxidative activity of isolated mitochondria. Increased AOX-dependent respiration was associated with heat generation under chilling stress using microcalorimetry (Ordentlich et al., 1991; Nevo et al., 1992; Moynihan et al., 1995). Although Breidenbach et al. (1997) stated that the enthalpy of mitochondrial respiration is not sufficient to cause physiologically relevant temperature increases in non-thermogenic plants, Grabelnych et al. (2003) suggested that the rapid shift from cytochrome *c* oxidase to AOX-dependent respiration opens a time window for the activation of protective mechanisms against low temperature stress. It is supported by the constant activity of antioxidant enzymes of *H. rhodopensis* during the chilling conditions (Georgieva at al., 2021). In conclusion, heat production of the increased mitochondrial activity through R_{alt} is significant under chilling stress conditions in *H. rhodopensis* that, over balancing the metabolism, might also enable the execution of temperature-dependent processes such as remodelling the vacuoles.

Under chilling stress, the majority of mitochondria were intruded into the vacuole in parallel to the increase in AOX activity (Fig. 4). Vesicles observed around the mitochondrial structures suggesting that these mitochondria are the subject of degradation by mitophagy. Mitophagy and mitophagy-specific cargo receptors were confirmed in plants in the recent years (Nakamura et al., 2021). We suggest the progression of the mitochondrial degradation as illustrated on Fig. 8 by proposed transition between the observed mitochondrial arrangements/mitochondria intruded into the vacuoles and subjects of mitophagy. The observed long chains of mitochondria that seemingly were present in multiple cross sections on transmission electron micrographs, and thus resembles the shape of immersion heater, represent elongated/fused mitochondria that intruded into the central vacuole (Fig. 8A) that structures were also discernible for longer time when the chilling stress period lasted longer in the given year. Mitochondria that were intruded into the vacuole were tagged with electron dense plaques. These plaques might represent joining areas connecting the organelles and contribute to the formation of a mitochondrial network associated with mitophagy (Frank et al., 2012). Cytosolic protein FRIENDLY (FMT) controls inter-mitochondrial associations induced by abiotic stresses. Putative proteins interacting with FMT contribute to the plaque formation (El-Zawily et al., 2014). Moreover, FMT also have a pivotal role in the depolarization induced mitophagy (Ma et al., 2021). Along with the elongated chains of mitochondria, the mitochondrial structures that show circular shape might represent sections of cup or doughnut shape mitochondria (Zhou et al., 2020; Otegui et al., 2024). Although we have not observed any differences in the external membrane disintegration, samples collected in the later stage of chilling conditions showed the signs of mitochondrial disorganization, i.e. fusion of cristae that form a central vesicle, and their total disappearance

was observed (Fig. 8B-D), that phenomenon was also reported from animal cells (Cereghetti and Scorrano, 2006). Detachment of the cristae at the junctions was suggested to be part of the degradation of the mitochondrial genome (He et al., 2022). Therefore, these mitochondria are seemingly also subject to degradation, and their degradation is delayed/might only completed upon exposition to sub-zero temperatures. Mitophagy is generally triggered by the depolarisation of the mitochondrial inner membrane (Duckney et al., 2024). Since the activity of AOX is electroneutral, and under succinate oxidation supported respiration, AOX does not effective in maintaining transmembrane membrane potential (Yoval-Sánchez et al., 2024), we suggest that high AOX activity also enhances the vulnerability of mitochondria to depolarisation in plants. Juárez et al. (2006) also indicated that shifting from cytochrome *c* dependent to alternative oxidase mediated respiration resulted in transient depolarisation in the fungus *Ustilago maydis*.

Summing up our results, we suggest that the not yet disintegrated mitochondria that have been already internalised in the vacuole during the chilling stress period still contribute to R_{alt} and can retain metabolic activity since malate/citrate transporters are also present in the tonoplast (Martinoia, 2018). The sequestration of the majority of mitochondria into the vacuole may give an additional advantage of protection against ROS accumulation in the mesophyll cells. In samples collected after the exposure to sub-zero conditions, when the cell content highly rearranges resembling the desiccated stage of *H. rhodopensis* (Mihailova et al. 2020), only cytoplasmic mitochondria were seen, while disintegrating mitochondria in the vacuole disappeared indicating the completing of mitophagy. The disappearance of the immersion heater like mitochondria together with the decreased R_{alt}, the lowered amount of AOX proteins and the elimination of the temperature difference between the leaves and the environment underlines the importance of these mitochondria in the AOX activity. While multiple chilling stress tolerant plant species were shown to alter the size, the number and the shape of mitochondria under chilling conditions (Kratsch and Wise, 2000, Venzhik et al., 2023), no vacuolar internalisation was reported so far in response to low temperature stresses. The mitochondria of *Arabidopsis thaliana* remain in the cytoplasm during cold acclimation at 4 °C (Ristic and Ashworth, 1993). Therefore, the vacuole internalisation of the immersion heater-like mitochondria during the chilling stress period is specific to *H. rhodopensis*, and contribute to its chilling tolerance.

Authors' contribution

Conceptualization: ÁK, ÉS, ÁS; Data curation and Formal analysis: ÁK, ÉS, IV, ÁS; Funding acquisition and Project administration: KG, IV, ÁS; Investigation: ÁK, ÉS, PN, H-DP, GM, GS, LS, KG, IV, ÁS; Methodology and Resources: ÁK, ÉS, PN, GS, IV, ÁS; Visualization: ÁS; Writing – original draft: ÁK, ÉS, ÁS; Writing – review and editing: all Authors.

Acknowledgement

The authors thank Katalin Solymosi for the computer graphics, Rudolf Solti for recording the environmental parameters, Tünde Szabó-Szöllősi (Botanical Garden, Eötvös Loránd University) for cultivation *Haberlea rhodopensis* plants in the *ex-situ* collection for protected plants, and Zsófia Gáti, Sándorné Pardi and Csilla Gergely for technical assistance in the molecular biology, protein, and electron microscopy laboratories, respectively.

Funding

This work was supported by the grant K-146865 of National Research, Development and Innovation Office, Hungary, and by the bilateral mobility grant between the Hungarian Academy of Sciences (HAS) and the Bulgarian Academy of Sciences (NKM 2023-57; and IC-HU/03/2024–2025, respectively). Á.S. was supported by the János Bolyai Scholarship of the HAS under grant number BO-00113-23-8.

Supplementary Data 1. Recorded environmental temperature data (daily minimum, daily maximum and average temperatures in °C) in the winter 2013/2014, 2014/2015, 2015/2016, and 2016/2017

Supplementary Data 2. Plotted night-time minimum, day-time maximum, and daily average temperatures with an indication of the sampling days in the winter 2013/2014, 2014/2015, and 2015/2016.

References

Barócsi A., Lenk S., Kocsányi L., Buschmann C. (2009) Excitation kinetics during induction of chlorophyll a fluorescence. *Photosynthetica*, 47, 104-111.

Benina, M., Obata, T., Mehterov, N., Ivanov, I., Petrov, V., Toneva, V., ... & Gechev, T. S. (2013). Comparative metabolic profiling of *Haberlea rhodopensis*, *Thellungiella halophyla*,

and *Arabidopsis thaliana* exposed to low temperature. *Frontiers in Plant Science*, 4, 499. https://doi.org/10.3389/fpls.2013.00499

Breidenbach, R. W., Saxton, M. J., Hansen, L. D., & Criddle, R. S. (1997). Heat generation and dissipation in plants: can the alternative oxidative phosphorylation pathway serve a thermoregulatory role in plant tissues other than specialized organs? *Plant Physiology*, 114, 1137-1140. https://doi.org/10.1104/pp.114.4.1137

Broda, M., Millar, A. H., & Van Aken, O. (2018). Mitophagy: a mechanism for plant growth and survival. *Trends in Plant Science*, *23*, 434-450. https://doi.org/10.1016/j.tplants.2018.02.010

Cereghetti, G. M., & Scorrano, L. (2006). The many shapes of mitochondrial death. *Oncogene*, 25, 4717-4724. https://doi.org/10.1038/sj.onc.1209605

Cheng, D. D., & Zhang, L. T. (2021). Mitochondrial alternative oxidase pathway acts as an electron sink during photosynthetic induction in Rumex K-1 leaves. *Photosynthetica*, 59, 615-624. https://doi.org/10.32615/ps.2021.047

Clifton, R., Lister, R., Parker, K. L., Sappl, P. G., Elhafez, D., Millar, A. H., ... & Whelan, J. (2005). Stress-induced co-expression of alternative respiratory chain components in *Arabidopsis thaliana*. *Plant Molecular Biology*, 58, 193-212. https://doi.org/10. 1103-005-5514-7

Considine, M. J., & Foyer, C. H. (2023). Metabolic regulation of quiescence in plants. *The Plant Journal*, 114, 1132-1148. https://doi.org/10.1111/tpj.16216

Cvetkovska, M., & Vanlerberghe, G. C. (2012). Coordination of a mitochondrial superoxide burst during the hypersensitive response to bacterial pathogen in *Nicotiana tabacum*. *Plant, Cell & Environment*, 35, 1121-1136. https://doi.org/10.1111/j.1365-3040.2011.02477.x

Del-Saz, N. F., Ribas-Carbo, M., McDonald, A. E., Lambers, H., Fernie, A. R., & Florez-Sarasa, I. (2018). An in vivo perspective of the role (s) of the alternative oxidase pathway. *Trends in Plant Science*, 23, 206-219. https://doi.org/10.1016/j.tplants.2017.11.006

Duckney, P. J., Wang, P., & Hussey, P. J. (2025). Mitophagy in plants: emerging regulators of mitochondrial targeting for selective autophagy. *Journal of Microscopy*, 297, 325-332. https://doi.org/10.1111/jmi.13267

El Zawily, A. M., Schwarzländer, M., Finkemeier, I., Johnston, I. G., Benamar, A., Cao, Y., ... & Logan, D. C. (2014). FRIENDLY regulates mitochondrial distribution, fusion, and quality control in Arabidopsis. *Plant Physiology*, 166, 808-828. https://doi.org/10.1104/pp.114.243824

Fedoseeva, I. V., Gamburg, K. Z., Varakina, N. N., Rusaleva, T. M., Tauson, E. L., Stupnikova, I. V., ... & Voinikov, V. K. (2008). The effect of sodium azide and 2, 4-dinitrophenol on the development of thermotolerance and induction of Hsp101 in cultured *Arabidopsis thaliana* cells. *Russian Journal of Plant Physiology*, 55, 225-231. https://doi.org/10.1134/S102144370802009X

Frank, M., Duvezin-Caubet, S., Koob, S., Occhipinti, A., Jagasia, R., Petcherski, A., ... & Reichert, A. S. (2012). Mitophagy is triggered by mild oxidative stress in a mitochondrial fission dependent manner. *Biochimica et Biophysica Acta (BBA)-Molecular Cell Research*, 1823, 2297-2310. https://doi.org/10.1016/j.bbamcr.2012.08.007

Gechev, T. S., Benina, M., Obata, T., Tohge, T., Sujeeth, N., Minkov, I., ... & Toneva, V. (2013). Molecular mechanisms of desiccation tolerance in the resurrection glacial relic *Haberlea rhodopensis*. *Cellular and Molecular Life Sciences*, 70, 689-709. https://doi.org/10.1007/s00018-012-1155-6

Georgieva, K., Rapparini, F., Bertazza, G., Mihailova, G., Sárvári, É., Solti, Á., & Keresztes, Á. (2017). Alterations in the sugar metabolism and in the vacuolar system of mesophyll cells contribute to the desiccation tolerance of *Haberlea rhodopensis* ecotypes. *Protoplasma*, 254, 193-201. https://doi.org/10.1007/s00709-015-0932-0

Georgieva, K., Mihailova, G., Velitchkova, M., & Popova, A. (2020). Recovery of photosynthetic activity of resurrection plant Haberlea rhodopensis from drought-and freezing-induced desiccation. *Photosynthetica*, 58. 911-921. https://doi.org/10.32615/ps.2020.044

Georgieva, K., Mihailova, G., Gigova, L., Dagnon, S., Simova-Stoilova, L., & Velitchkova, M. (2021). The role of antioxidant defense in freezing tolerance of resurrection plant *Haberlea rhodopensis*. *Physiology and Molecular Biology of Plants*, 27, 1119-1133. https://doi.org/10.1007/s12298-021-00998-0

Georgieva, K., Mihailova, G., Fernández-Marín, B., Bertazza, G., Govoni, A., Arzac, M. I., ... & Rapparini, F. (2022). Protective strategies of *Haberlea rhodopensis* for acquisition of

freezing tolerance: Interaction between dehydration and low temperature. *International Journal of Molecular Sciences*, 23, 15050. https://doi.org/10.3390/ijms232315050

Grabelnych, O. I., Kolesnichenko, A. V., Pobezhimova, T. P., Tourchaninova, V. V., Korzun, A. M., Koroleva, N. A., ... & Voinikov, V. K. (2003). The role of different plant seedling shoots mitochondrial uncoupling systems in thermogenesis during low-temperature stress. *Journal of Thermal Biology*, 28, 571-580. https://doi.org/10.1016/j.jtherbio.2003.08.003

Grabelnych, O. I., Borovik, O. A., Tauson, E. L., Pobezhimova, T. P., Katyshev, A. I., Pavlovskaya, N. S., ... & Voinikov, V. K. (2014). Mitochondrial energy-dissipating systems (alternative oxidase, uncoupling proteins, and external NADH dehydrogenase) are involved in development of frost-resistance of winter wheat seedlings. *Biochemistry (Moscow)*, 79, 506-519. https://doi.org/10.1134/S0006297914060030

He, B., Yu, H., Liu, S., Wan, H., Fu, S., Liu, S., ... & Jiang, H. (2022). Mitochondrial cristae architecture protects against mtDNA release and inflammation. *Cell Reports*, 41, 111774. https://doi.org/10.1016/j.celrep.2022.111774

Heidarvand, L., Millar, A. H., & Taylor, N. L. (2017). Responses of the mitochondrial respiratory system to low temperature in plants. *Critical Reviews in Plant Sciences*, 36, 217-240. https://doi.org/10.1080/07352689.2017.1375836

Hendrickson, C., Hewitt, S., Swanson, M. E., Einhorn, T., & Dhingra, A. (2019). Evidence for pre-climacteric activation of AOX transcription during cold-induced conditioning to ripen in European pear (*Pyrus communis* L.). *PloS One*, 14, e0225886. https://doi.org/10.1371/journal.pone.0225886

Ho, L. H., Giraud, E., Lister, R., Thirkettle-Watts, D., Low, J., Clifton, R., ... & Whelan, J. (2007). Characterization of the regulatory and expression context of an alternative oxidase gene provides insights into cyanide-insensitive respiration during growth and development. *Plant Physiology*, 143, 1519-1533. https://doi.org/10.1104/pp.106.091819

Ho L.H.M., Giraud E., Uggalla V., Lister R., Clifton R., Glen A., Thirkettle-Watts D., Van Aken O. & Whelan J. (2008) Identification of regulatory pathways controlling gene expression of stress-responsive mitochondrial proteins in Arabidopsis. *Plant Physiology* 147, 1858–1873. https://doi.org/10.1104/pp.108.121384

Hoekstra, F. A., Golovina, E. A., & Buitink, J. (2001). Mechanisms of plant desiccation tolerance. *Trends in Plant Science*, 6, 431-438. https://doi.org/10.1016/S1360-1385(01)02052-0

Igamberdiev, A. U. (2020). Citrate valve integrates mitochondria into photosynthetic metabolism. *Mitochondrion*, 52, 218-230. https://doi.org/10.1016/j.mito.2020.04.003

Ivanova, A., O′ Leary, B., Signorelli, S., Falconet, D., Moyankova, D., Whelan, J., ... & Murcha, M. W. (2022). Mitochondrial activity and biogenesis during resurrection of *Haberlea rhodopensis*. *New Phytologist*, 236, 943-957. https://doi.org/10.1111/nph.18396

Jiang, Y., Nie, Y., Pan, Y., Li, X., Liu, H., & Tao, S. (2023). Enhanced cyanide-resistant respiration as the predominant respiratory metabolic pathway in abnormal chilling injury behavior of postharvest papaya. *Postharvest Biology and Technology*, 205, 112505. https://doi.org/10.1016/j.postharvbio.2023.112505

Juárez, O., Guerra, G., Velázquez, I., Flores-Herrera, O., Rivera-Pérez, R. E., & Pardo, J. P. (2006). The physiologic role of alternative oxidase in *Ustilago maydis*. *The FEBS Journal*, *273*, 4603-4615. https://doi.org/10.1111/j.1742-4658.2006.05463.x

Kacprzak, S. M., & Van Aken, O. (2022). Carbon starvation, senescence and specific mitochondrial stresses, but not nitrogen starvation and general stresses, are major triggers for mitophagy in Arabidopsis. *Autophagy*, *18*, 2894-2912. https://doi.org/10.1080/15548627.2022.2054039

Kaňa, R., & Vass, I. (2008). Thermoimaging as a tool for studying light-induced heating of leaves: Correlation of heat dissipation with the efficiency of photosystem II photochemistry and non-photochemical quenching. *Environmental and Experimental Botany*, 64, 90-96. https://doi.org/10.1016/j.envexpbot.2008.02.006

Karami-Moalem, S., Maali-Amiri, R., & Kazemi-Shahandashti, S. S. (2018). Effect of cold stress on oxidative damage and mitochondrial respiratory properties in chickpea. *Plant Physiology and Biochemistry*, 122, 31-39. https://doi.org/10.1016/j.plaphy.2017.11.011

Kratsch, H. A., Wise, R.R (2000). The ultrastructure of chilling stress. *Plant Cell and Environment*, 23, 337-350. The ultrastructure of chilling stress

Laemmli, U. K. (1970). Cleavage of structural proteins during the assembly of the head of bacteriophage T4. *Nature*, 227, 680-685. https://doi.org/10.1038/227680a0

Lamprecht, I., Schmolz, E., Blanco, L., & Romero, C. M. (2002). Flower ovens: thermal investigations on heat producing plants. *Thermochimica Acta*, 391, 107-118. https://doi.org/10.1016/S0040-6031(02)00168-5

Laxa, M., Liebthal, M., Telman, W., Chibani, K., & Dietz, K. J. (2019). The role of the plant antioxidant system in drought tolerance. *Antioxidants*, 8, 94. https://doi.org/10.3390/antiox8040094

Legardón, A., & García-Plazaola, J. I. (2023). Gesneriads, a source of resurrection and double-tolerant species: proposal of new desiccation-and freezing-tolerant plants and their physiological adaptations. Biology, 12, 107. https://doi.org/10.3390/biology12010107

Li, C. R., Liang, D. D., Xu, R. F., Li, H., Zhang, Y. P., Qin, R. Y., ... & Yang, J. B. (2013). Overexpression of an alternative oxidase gene, *OsAOX1a*, improves cold tolerance in *Oryza sativa* L. *Genetics and Molecular Research*, 12, 5424-5432. https://doi.org/10.4238/2013.November.11.4.

Luong, A. M., Koestel, J., Bhati, K. K., & Batoko, H. (2022). Cargo receptors and adaptors for selective autophagy in plant cells. *FEBS Letters*, 596, 2104-2132. https://doi.org/10.1002/1873-3468.14412

Ma, J., Liang, Z., Zhao, J., Wang, P., Ma, W., Mai, K. K., ... & Kang, B. H. (2021). Friendly mediates membrane depolarization-induced mitophagy in Arabidopsis. *Current Biology*, 31, 1931-1944. https://doi.org/10.1016/j.cub.2021.02.034

Mathur, S., Agrawal, D., & Jajoo, A. (2014). Photosynthesis: response to high temperature stress. *Journal of Photochemistry and Photobiology B: Biology*, 137, 116-126. https://doi.org/10.1016/j.jphotobiol.2014.01.010

Martinoia, E. (2018). Vacuolar transporters–companions on a longtime journey. *Plant Physiology*, 176, 1384-1407. https://doi.org/10.1104/pp.17.01481

Meeuse, B. J. (1975). Thermogenic respiration in aroids. *Annual Review of Plant Physiology*, 26, 117-126. https://doi.org/10.1146/annurev.pp.26.060175.001001

Mihailova, G., Solti, Á., Sárvári, É., Keresztes, Á., Rapparini, F., Velitchkova, M., ... & Georgieva, K. (2020). Freezing tolerance of photosynthetic apparatus in the homoiochlorophyllous resurrection plant *Haberlea rhodopensis*. *Environmental and Experimental Botany*, 178, 104157. https://doi.org/10.1016/j.envexpbot.2020.104157

Mihailova, G., Vasileva, I., Gigova, L., Gesheva, E., Simova-Stoilova, L., & Georgieva, K. (2022). Antioxidant defense during recovery of resurrection plant *Haberlea rhodopensis* from drought-and freezing-induced desiccation. *Plants*, 11, 175. https://doi.org/10.3390/plants11020175

Mihailova, G., Gashi, B., Krastev, N., & Georgieva, K. (2023). Acquisition of freezing tolerance of resurrection species from Gesneriaceae, a comparative study. *Plants*, 12, 1893. https://doi.org/10.3390/plants12091893

Miller, R. E., Grant, N. M., Giles, L., Ribas-Carbo, M., Berry, J. A., Watling, J. R., & Robinson, S. A. (2011). In the heat of the night–alternative pathway respiration drives thermogenesis in *Philodendron bipinnatifidum*. *New Phytologist*, 189, 1013-1026. https://doi.org/10.1111/j.1469-8137.2010.03547.x

Minibayeva, F., Dmitrieva, S., Ponomareva, A., & Ryabovol, V. (2012). Oxidative stress-induced autophagy in plants: the role of mitochondria. *Plant Physiology and Biochemistry*, 59, 11-19. https://doi.org/10.1016/j.plaphy.2012.02.013

Mladenov, P., Zasheva, D., Planchon, S., Leclercq, C. C., Falconet, D., Moyet, L., ... & Deng, X. (2022). Proteomics evidence of a systemic response to desiccation in the resurrection plant *Haberlea rhodopensis*. *International Journal of Molecular Sciences*, 23, 8520. https://doi.org/10.3390/ijms23158520

Moynihan, M. R., Ordentlich, A., & Raskin, I. (1995). Chilling-induced heat evolution in plants. *Plant Physiology*, 108, 995-999. https://doi.org/10.1104/pp.108.3.995

Mróz, T. L., Havey, M. J., & Bartoszewski, G. (2015). Cucumber possesses a single terminal alternative oxidase gene that is upregulated by cold stress and in the mosaic (MSC) mitochondrial mutants. *Plant Molecular Biology Reporter*, 33, 1893-1906. https://doi.org/10.1007/s11105-015-0883-9

Nakamura, S., Hagihara, S., Otomo, K., Ishida, H., Hidema, J., Nemoto, T., & Izumi, M. (2021). Autophagy contributes to the quality control of leaf mitochondria. *Plant and Cell Physiology*, 62, 229-247. https://doi.org/10.1093/pcp/pcaa162

Nevo, E., Ordentlich, A., Beiles, A., & Raskin, I. (1992). Genetic divergence of heat production within and between the wild progenitors of wheat and barley: evolutionary and agronomical implications. *Theoretical and Applied Genetics*, 84, 958-962. https://doi.org/10.1007/BF00227410

Ordentlich, A., Linzer, R. A., & Raskin, I. (1991). Alternative respiration and heat evolution in plants. *Plant Physiology*, 97, 1545-1550. https://doi.org/10.1104/pp.97.4.1545

Otegui, M. S., Steelheart, C., Ma, W., Ma, J., Kang, B. H., De Medina Hernandez, V. S., ... & Nishimura, M. (2024). Vacuolar degradation of plant organelles. *The Plant Cell*, *36*, 3036-3056. https://doi.org/10.1093/plcell/koae128

Pál, M. Horváth, E., Janda, T., Páldi, E., Szalai, G. (2005) Cadmium stimulates the accumulation of salicylic acid and its putative precursors in maize (Zea mays) plants. Physiologia Plantarum, 125(3), o. 356–364. https://doi.org/10.1111/j.1399-3054.2005.00545.x.

Petersen, M., Avin-Wittenberg, T., Bassham, D. C., Dagdas, Y., Fan, C., Fernie, A. R., ... & Hofius, D. (2024). Autophagy in plants. *Autophagy Reports*, *3*, 2395731. https://doi.org/10.1080/27694127.2024.2395731

Pfaffl, M.W. (2001). A new mathematical model for relative quantification in real-time RT-PCR. *Nucleic Acids Research*, 29, 2002-2007. https://doi.org/10.1093/nar/299e45

Pham, H. M., Kebede, H., Ritchie, G., Trolinder, N., & Wright, R. J. (2018). Alternative oxidase (AOX) over-expression improves cell expansion and elongation in cotton seedling exposed to cool temperatures. *Theoretical and Applied Genetics*, 131, 2287-2298. https://doi.org/10.1007/s00122-018-3151-1

Pu, X., Lv, X., Tan, T., Fu, F., Qin, G., & Lin, H. (2015). Roles of mitochondrial energy dissipation systems in plant development and acclimation to stress. *Annals of Botany*, 116, 583-60 https://doi.org/10.1093/aob/mcv063, 0

Ristic, Z., Ashworth, E. N. (1993). Changes in leaf ultrastructure and carbohydrates in *Arabidopsis thaliana* L. (Heyn) cv. Columbia during rapid cold acclimation. *Protoplasma* 172, 111-123. https://doi.org/10.1007/BF01379368

Rogov, A. G., Sukhanova, E. I., Uralskaya, L. A., Aliverdieva, D. A., & Zvyagilskaya, R. A. (2014). Alternative oxidase: distribution, induction, properties, structure, regulation, and functions. *Biochemistry (Moscow)*, 79, 1615-1634. https://doi.org/10.1134/S0006297914130112

Saha, B., Borovskii, G., & Panda, S. K. (2016). Alternative oxidase and plant stress tolerance. *Plant Signaling and Behavior*, 11, e1256530. https://doi.org/10.1080/15592324.2016.1256530

Schonbaum, G. R., Bonner Jr, W. D., Storey, B. T., & Bahr, J. T. (1971). Specific inhibition of the cyanide-insensitive respiratory pathway in plant mitochondria by hydroxamic acids. *Plant Physiology*, 47, 124-128. https://doi.org/10.1104/pp.47.1.124

Selinski, J., Scheibe, R., Day, D. A., & Whelan, J. (2018). Alternative oxidase is positive for plant performance. *Trends in Plant Science*, 23, 588-597. https://doi.org/10.1016/j.tplants.2018.03.012

Seyran M, Brenneman T.B., Stevenson K.L. (2010) In vitro toxicity of alternative oxidase inhibitors salicylhydroxamic acid and propyl gallate on Fusicladium effusum. Journal of Pesticide Science 83, 421-427.

Solti, Á., Lenk, S., Mihailova, G., Mayer, P., Barócsi, A., & Georgieva, K. (2014). Effects of habitat light conditions on the excitation quenching pathways in desiccating *Haberlea rhodopensis* leaves: an Intelligent FluoroSensor study. *Journal of Photochemistry and Photobiology B: Biology*, 130, 217-225. https://doi.org/10.1016/j.jphotobiol.2013.11.016

van Doorn, W. G., & Papini, A. (2013). Ultrastructure of autophagy in plant cells: a review. *Autophagy*, 9, 1922-1936. https://doi.org/10.4161/auto.26275

Vanlerberghe, G. C. (2013). Alternative oxidase: a mitochondrial respiratory pathway to maintain metabolic and signaling homeostasis during abiotic and biotic stress in plants. *International Journal of Molecular Sciences*, 14, 6805-6847. https://doi.org/10.3390/ijms14046805

Vanlerberghe, G. C., Dahal, K., Alber, N. A., & Chadee, A. (2020). Photosynthesis, respiration and growth: a carbon and energy balancing act for alternative oxidase. *Mitochondrion*, 52, 197-211. https://doi.org/10.1016/j.mito.2020.04.001

Venzhik, Y., Deryabin, A., & Moshkov, I. (2023). Adaptive strategy of plant cells during chilling: Aspect of ultrastructural reorganization. *Plant Science*, 332, 111722. https://doi.org/10.1016/j.plantsci.2023.111722

Verhoeven, A., García-Plazaola, J. I., & Fernández-Marín, B. (2018). Shared mechanisms of photoprotection in photosynthetic organisms tolerant to desiccation or to low temperature. *Environmental and Experimental Botany*, 154, 66-79. https://doi.org/10.1016/j.envexpbot.2017.09.012.

Vojnikov, V., Korzun, A., Pobezhimova, T., & Varakina, N. (1984). Effect of cold shock on the mitochondrial activity and on the temperature of winter wheat seedlings. *Biochemie und Physiologie der Pflanzen*, 179, 327-330. https://doi.org/10.1016/S0015-3796(84)80049-9

Wang, J., & Vanlerberghe, G. C. (2013). A lack of mitochondrial alternative oxidase compromises capacity to recover from severe drought stress. *Physiologia Plantarum*, 149, 461-473. https://doi.org/10.1111/ppl.12059

Wang, J., Rajakulendran, N., Amirsadeghi, S., & Vanlerberghe, G. C. (2011). Impact of mitochondrial alternative oxidase expression on the response of *Nicotiana tabacum* to cold temperature. *Physiologia Plantarum*, 142, 339-351. https://doi.org/10.1111/j.1399-3054.2011.01471.x

Yamada, Y., Suzuki, K., Yanagishita, H., & Noguchi, K. (2024). Roles of mitochondrial alternative oxidase in photosynthetic electron transport in illuminated leaves of *Arabidopsis thaliana* at low temperature. *Journal of Biosciences*, 49, 61. https://doi.org/10.1007/s12038-024-00446-7

Yamori, W., Hikosaka, K., & Way, D. A. (2014). Temperature response of photosynthesis in C3, C4, and CAM plants: temperature acclimation and temperature adaptation. *Photosynthesis Research*, *119*: 101-117. https://doi.org/10.1007/s11120-013-9874-6

Zhang, H., Zhou, S., Pristijono, P., Golding, J. B., Yang, H., Chen, G., & Li, Y. (2021). Role of AOX in low-temperature conditioning induced chilling tolerance in sweetpotato roots. *Scientia Horticulturae*, 288, 110365. https://doi.org/10.1016/j.scienta.2021.110365

Zhou, Y., Long, Q., Wu, H., Li, W., Qi, J., Wu, Y., ... & Liu, X. (2020). Topology-dependent, bifurcated mitochondrial quality control under starvation. *Autophagy*, 16, 562-574. https://doi.org/10.1080/15548627.2019.1634944

Zhu, T., Zou, L., Li, Y., Yao, X., Xu, F., Deng, X., ... & Lin, H. (2018). Mitochondrial alternative oxidase-dependent autophagy involved in ethylene-mediated drought tolerance in *Solanum lycopersicum*. *Plant Biotechnology Journal*, 16, 2063-2076. https://doi.org/10.1111/pbi.12939

Table 1. Oligonucleotide primers used in the expression analysis of mitochondrial alternative oxidase.

Gene	**contig**	***Arabidopsis* ortholog**	**Primer**	**Primer sequences**	**T_m (°C)**	**Product (bp)**
HrAOX2	*002889*	*At5g64210*	fw	5'- GCTGCCGTTCCTGGTATGGTA -3'	65.5	156
			rev	5'- CCACTTTGGCTGCACAAGCTC -3'		
HrHSP90	*000452*	*XP_002869603*	fw	5' - GTAAGAAACTCGTATCTGCTACC - 3'	60	160
			rev	5' - CGGCTAGAAACCACTACCT - 3'		
HrUBC5	*009712*	*At3g62250*	fw	5' - GCCGAAGAAGATCAAGCAC - 3'	60	121
			rev	5' - GCCGCACTCAAGATTAGG - 3'		

Table 2. Absolute minimum (abs. min.), absolute maximum (abs. max.), average minimum (average min.) and average maximum (average max.) temperature values of preceding 7-day time frame to sampling date, in each one of the experimental years. Minimum, maximum and average temperature values are indicated in °C. Regarding average temperatures, SD values are indicated.

	Winter 2013/2014				**Winter 2014/2015**				**Winter 2015/2016**				**Winter 2016/2017**			
	abs. min.	**abs. max.**	**average min.**	**average max.**	**abs. min**	**abs. max.**	**average min.**	**average max.**	**abs. min.**	**abs max.**	**average min.**	**average max.**	**abs. min.**	**abs. max.**	**average min.**	**average max.**
BS	8	23	9.6±1.1	19.3±2.4	13	25	13.4±0.5	21.9±2.9	5	21	9.3±3.6	19.0±1.5	8	23	12.2±2.6	17.6±4.2
CH	0	4	0.7±1.0	2.1±1.1	3	10	4.7±2.1	8.0±1.8	0	18	5.7±3.6	10.1±5.4				
CH-1													-3	7	1.3±2.4	5.4±1.0
CH-2													2	12	3.6±1.1	8.6±2.1
SZ	-8	1	-5.6±1.5	-1.0±1.3	-8	5	-3.4±2.4	-0.3±3.5	-8	5	-3.7±3.2	-0.9±3.2				
SZ-1													-4	5	-2.1±2.0	1.9±2.3
SZ-2													-3	10	-0.3±2.9	4.6±4.2
AS	6	22	9.6±2.1	18.0±2.6	5	23	7.9±2.7	19.4±2.7	9	23	11.0±1.7	20.3±2.8	4	22	6.6±2.0	15.9±3.4

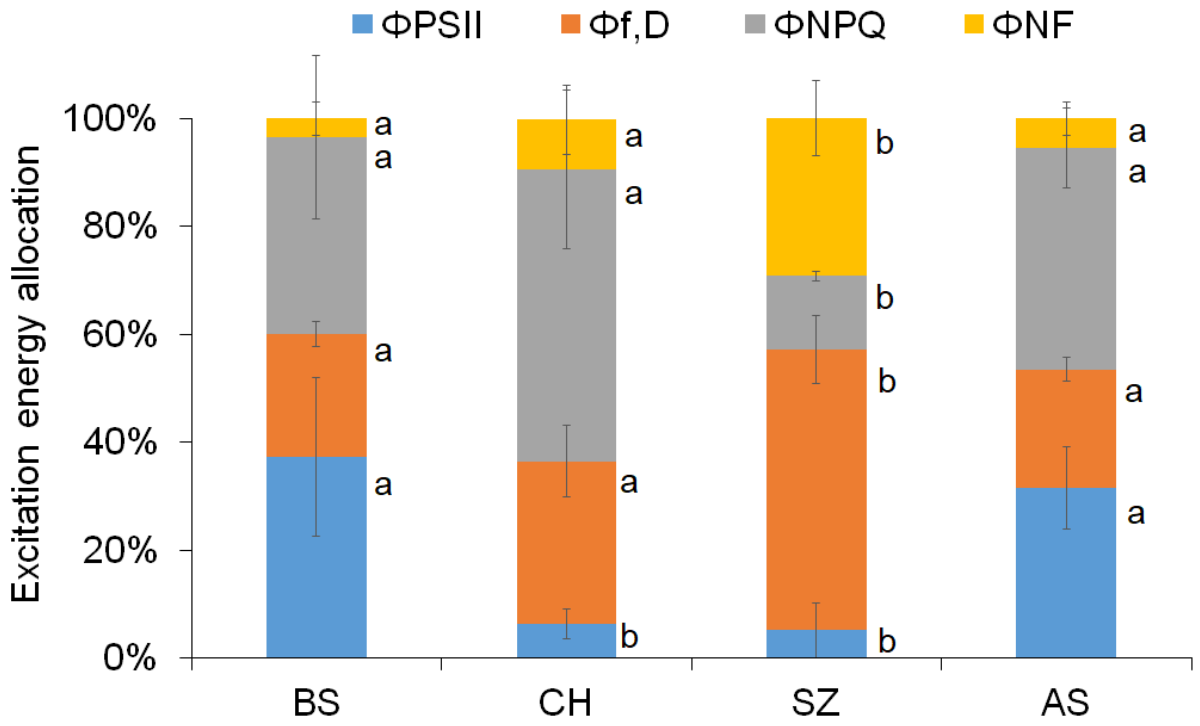

Figure 1. Excitation energy allocation in photosystem II reaction centres in samples collected before the temperature stresses (BS), under chilling conditions (CH), after being subjected to sub-zero temperatures (SZ) and after the temperature stresses (AS). Error bars represent SD values. To compare the differences regarding each separate parameter, one-way ANOVAs were performed with Tukey-Kramer *post-hoc* tests on the treatments ($P<0.05$; $n=6$). Statistical groups within each separate parameters are indicated by minuscule.

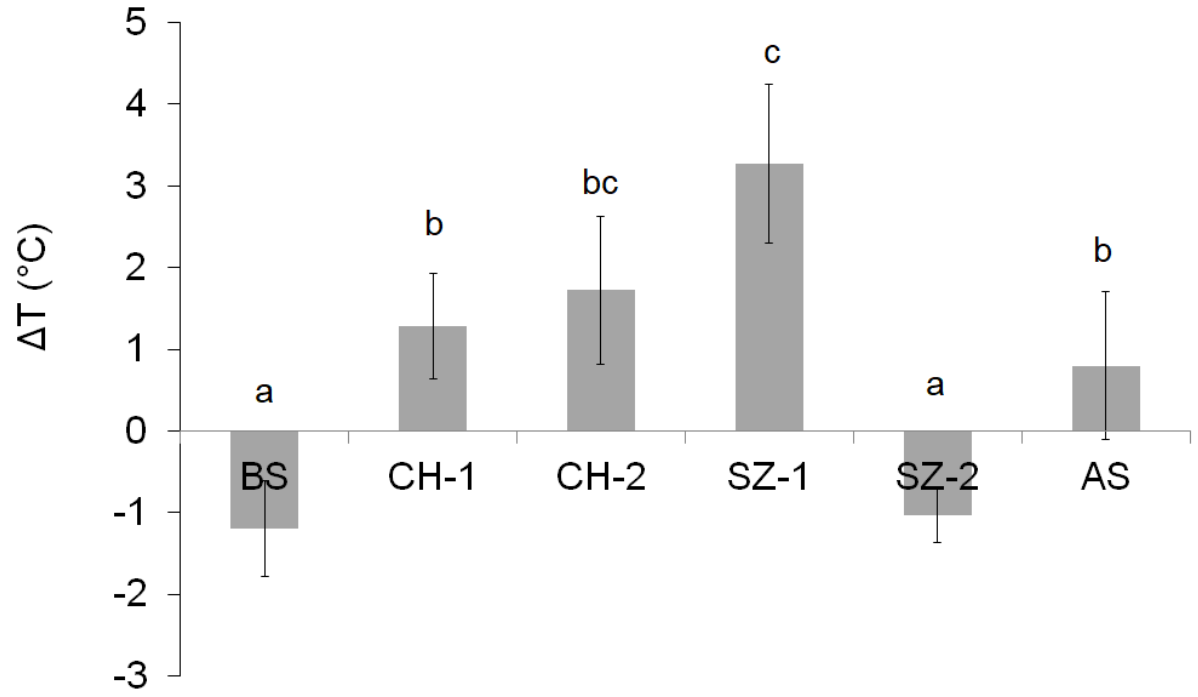

Figure 2. Difference of the temperature of leaves to the ambient temperature based on contact leaf thermometer measurements in a pilot experiment recorded before the temperature stresses (BS: 5/10/2016), under chilling conditions (CH-1: 17/11/2016; CH-2: 28/11/2016; CH-3: 8/12/2016), after subjected to sub-zero temperatures (SZ: 14/12/2016) and after the temperature stresses (AS: 22/3/2017). Error bars represent SD values. To compare the differences, one-way ANOVAs were performed with Tukey-Kramer *post-hoc* tests on the treatments (P<0.05; n=6). Statistical groups are indicated by minuscule.

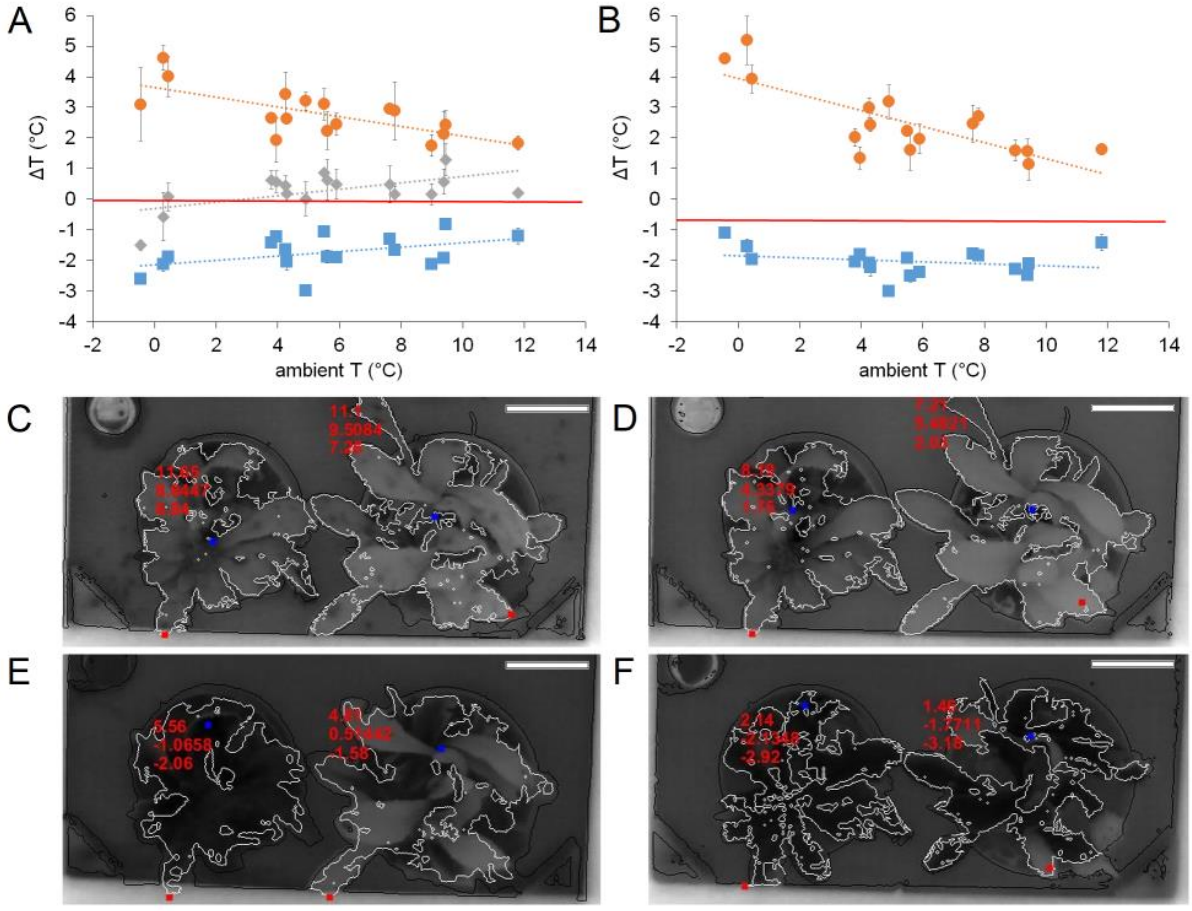

Figure 3. Alteration in the temperature of leaves at different environmental temperature conditions. (**A**) Alterations of minimum (blue square), average (grey diamond), and maximum (orange dot) temperatures of the leaf blades of the temperature of the environment that surround the plant individuals recorded by remote thermocamera measurements. Dotted lines represent linear fits on the datasets, red solid line indicate 0 °C temperature alteration; (**B**) deviation of maximum (orange dot) and minimum (blue square) temperatures of the average leaf lamina temperature values. Dotted lines represent linear fits on the datasets, red solid line indicate 0 °C temperature alteration; (**C**-**F**) Thermocamera images were recorded at (**C**) 9.023, (**D**) 4.923, (**E**) 0.283, and (**F**) -0.457 °C ambient temperature conditions. Blue and red dots indicate the location of minimum and maximum temperature pixels. Bars are 5 cm on (**C**-**F**).

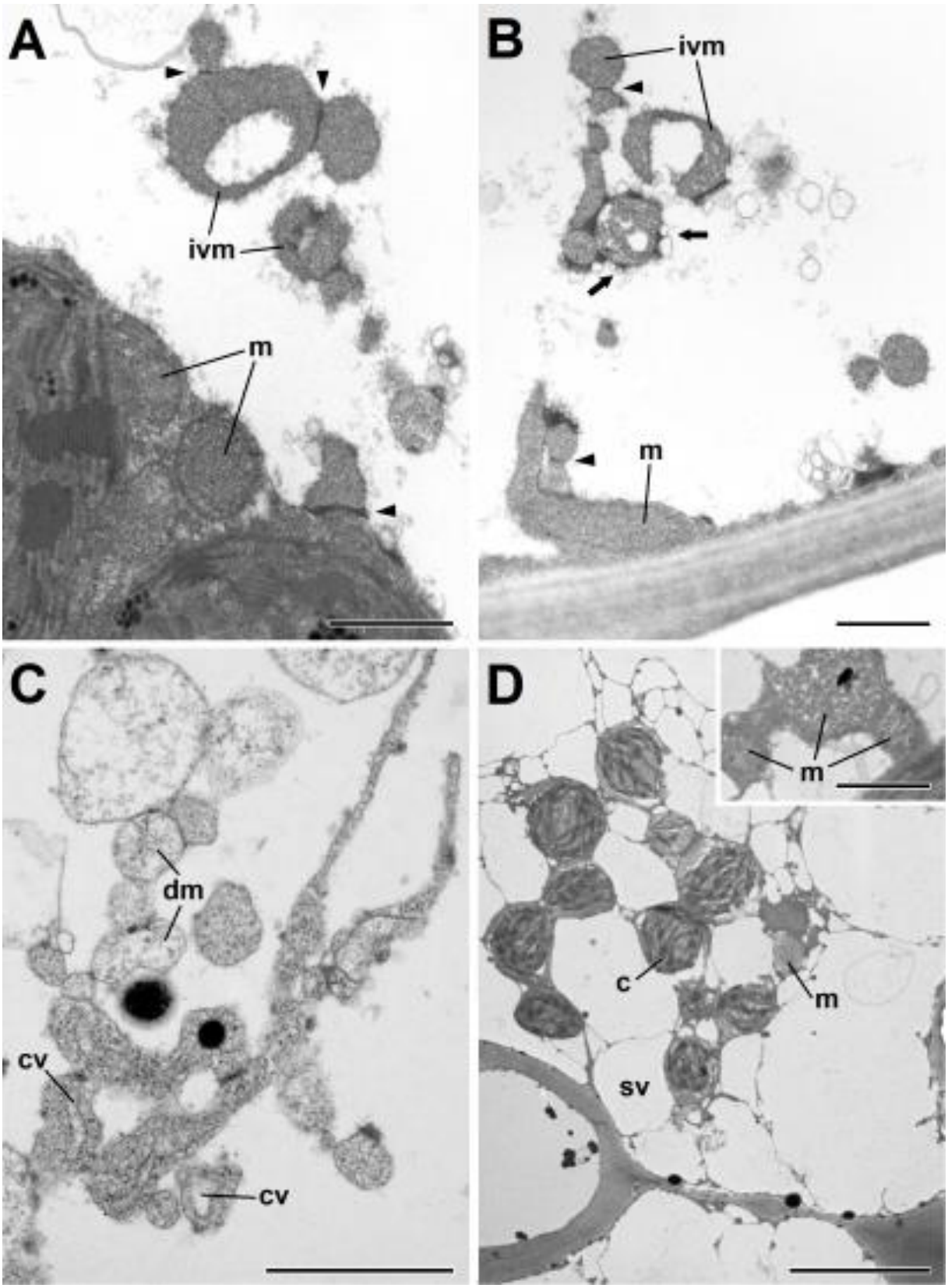

Figure 4. Arrangement of organelles in the mesophyll cells under chilling (**A-C**) and after exposure to sub-zero (**D**) conditions. **A**: Mitochondria intruding into the vacuole are often attached to each other by dense layers. **B**: Mitochondria in the vacuole may be roundish, cup-shaped or elongated surrounded by small vesicles. **C**: A part of intravacuolar mitochondria

eventually become very deformed, and contain vesicles probably representing the remnants of the inner membrane, while many of them show symptoms of degradation. **D**: In samples collected after exposure to sub-zero temperatures the organelles are found in central position associated with larger peripheral secondary vacuoles, the cytoplasmic mitochondria among the chloroplasts are not degraded (inset). Abbreviations: cv – coalescent inner membrane vesicles, dm − degrading mitochondria, ivm −intravacuolar mitochondria, m − mitochondria in the cytoplasm, sv −secondary vacuole, arrowheads mark the dense layer, arrows point to vesicles probably originating from the tonoplast. Bars are 2 µm on (**A**), (**B**), (**C**), and (**D**) inset; and 10 µm on (**D**).

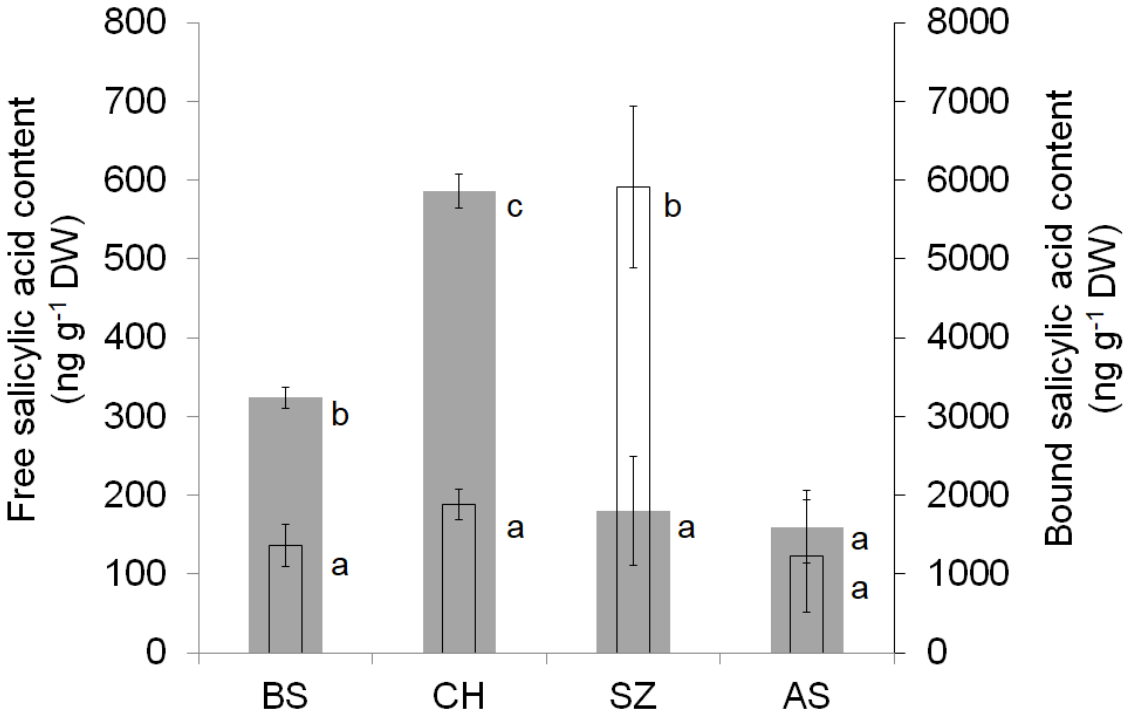

Figure 5. Changes in the free (closed columns) and bound (open columns) salicylic acid content in samples collected before the temperature stresses (BS), under chilling conditions (CH), after being subjected to sub-zero temperatures (SZ), and after the temperature stresses (AS). Error bars represent SD values. To compare the differences regarding each separate parameter, one-way ANOVAs were performed with Tukey-Kramer *post-hoc* tests on the treatments ($P<0.05$; $n=3$). Statistical groups within each separate parameters are indicated by minuscule.

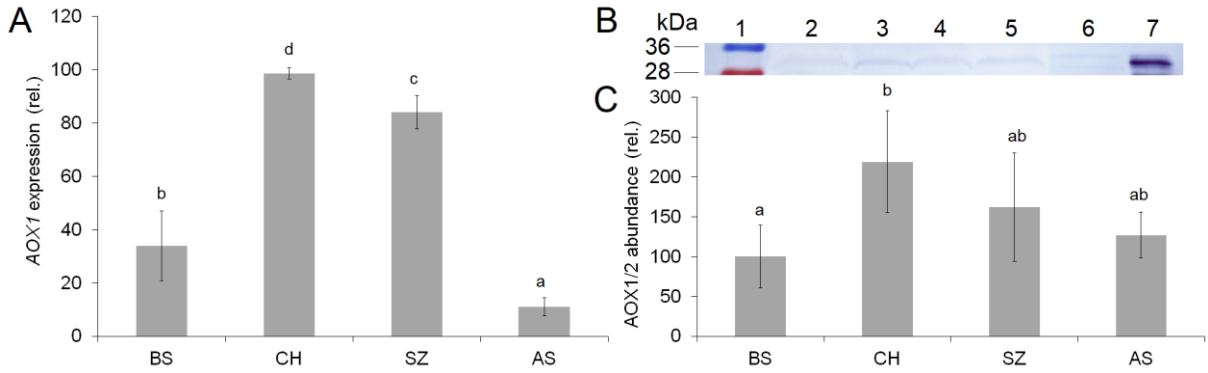

Figure 6. (**A**) Normalised relative transcript abundance of *HrAOX2* in samples collected before the temperature stresses (BS), under chilling conditions (CH), after being subjected to sub-zero temperatures (SZ), and after the temperature stresses (AS). Error bars represent SD values. To compare the differences, one-way ANOVAs were performed with Tukey-Kramer *post-hoc* tests on the treatments (P<0.05; n=9). (**B, C**) Changes in the protein amount of the mitochondrial alternative oxidase. (**B**) Representative figure of immunoblot against AOX 1/2. Loaded samples were: (**1**) PageRuler™ Plus Prestained Protein Ladder (Thermo-Fisher Scientific; Lot.: 00463463); *H. rhodopensis* total leaf proteins isolated from control plants in autumn under normal temperature (**2**), in wintertime under cold (**3**) and freezing (**4**) temperature and in spring under warming up (**5**); *Arabidopsis thaliana* total leaf proteins isolated from cold treated plants (**6**); *Typhonium venosum* inflorescence synandrium total proteins (**7**). Lanes on immunoblots were loaded with 75 µg solubilised protein. (**C**) Cumulative relative protein content of *H. rhodopensis* mitochondrial AOX 1 and 2 in samples collected before the temperature stresses (BS), under chilling conditions (CH), after being subjected to sub-zero temperatures (SZ) and after the temperature stresses (AS). Error bars represent SD values. To compare the differences regarding each separate parameter, one-way ANOVAs were performed with Tukey-Kramer *post-hoc* tests on the treatments (P<0.05; n=9). Statistical groups within each separate parameters are indicated by minuscule.

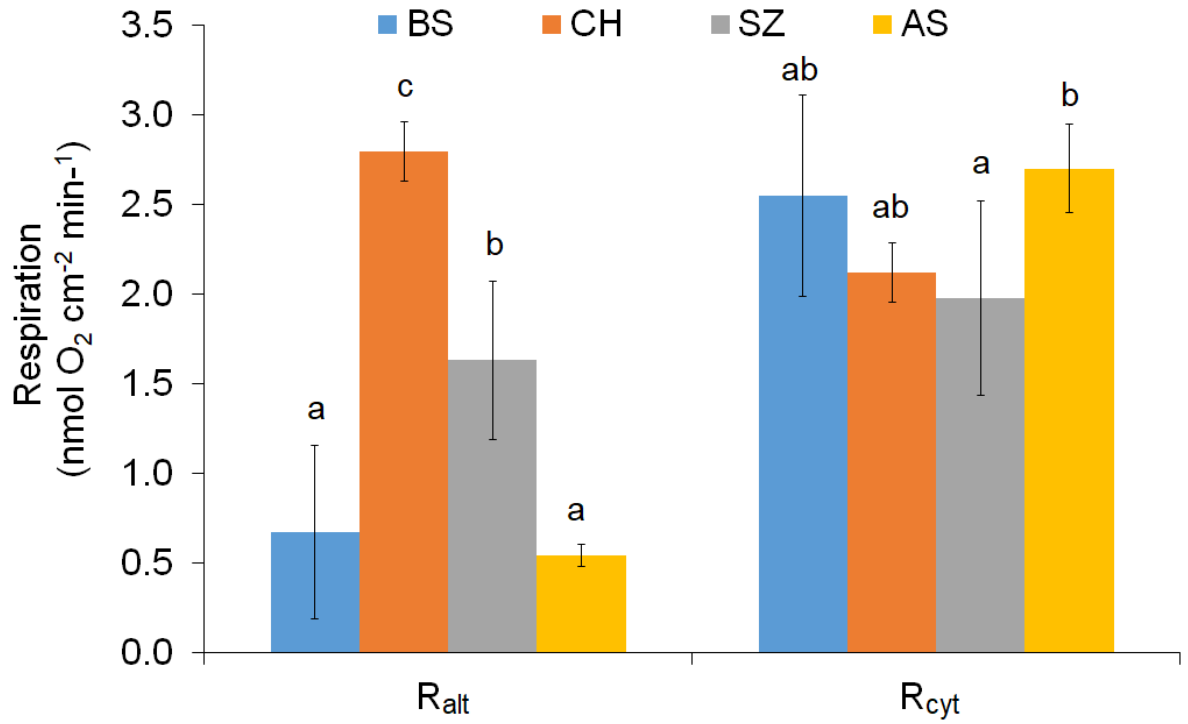

Figure 7. Contribution of the cytochrome *c* oxidase dependent (R_{cyt}) and AOX-dependent alternative terminal oxidation (R_{alt}) pathways to the oxygen consumption in samples collected before the temperature stresses (BS), under chilling conditions (CH), after being subjected to sub-zero temperatures (SZ) and after the temperature stresses (AS). Error bars represent SD values. To compare the differences regarding each separate parameter, one-way ANOVAs were performed with Tukey-Kramer *post-hoc* tests on the treatments (P<0.05; n=6). Statistical groups within each separate parameters are indicated by minuscule.

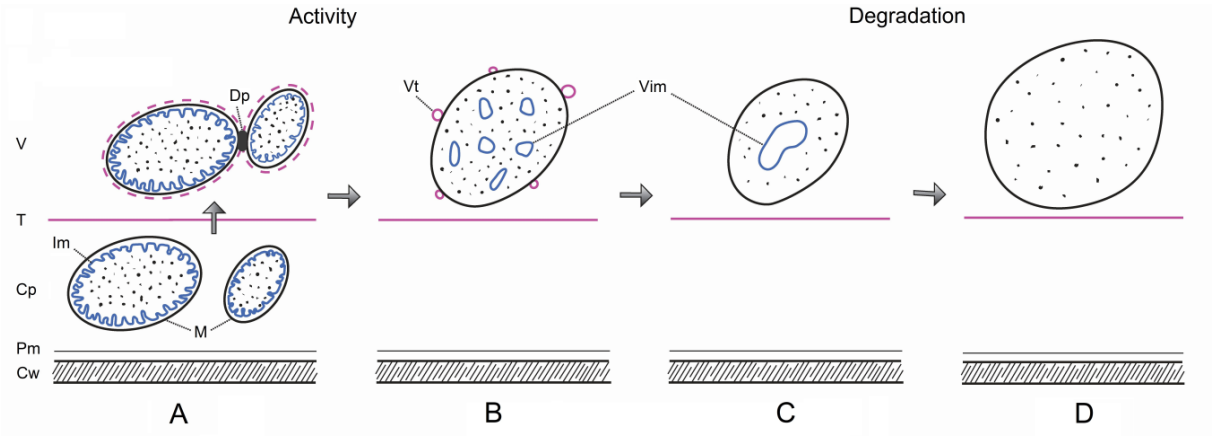

Figure 8. Suggested progression of mitochondria in the mesophyll cells from early (**A**) to late (**D**) chilling stress conditions, where intermediate step (**B**) and (**C**) are proposed transition structures between the observed arrangements of mitochondria. Abbreviations: Cp – cytoplasm; Cw – cell wall; Dp – dense plaque; Im – inner membrane; M – mitochondrion; Pm – plasma

membrane; T – tonoplast; V – vacuole; Vim – vesiculated inner membrane; Vt – vesiculated tonoplast.